Renewable and Sustainable Energy Reviews 33 (2014) 177–187

Contents lists available at ScienceDirect

Renewable and Sustainable Energy Reviews

journal homepage: www.elsevier.com/locate/rser

A review of full-scale structural testing of wind turbine blades

H.F. Zhou [a,*], H.Y. Dou [a], L.Z. Qin [a], Y. Chen [b], Y.Q. Ni [b], J.M. Ko [b]

[a] *College of Architecture and Civil Engineering, Wenzhou University, Chashan University Town, Wenzhou 325035, China*
[b] *Department of Civil and Environmental Engineering, The Hong Kong Polytechnic University, Hung Hom, Kowloon, Hong Kong*

ARTICLE INFO

Article history:
Received 14 August 2013
Received in revised form
21 November 2013
Accepted 31 January 2014
Available online 25 February 2014

Keywords:
Wind turbine blade
Structural testing
Photogrammetry
Digital image correlation
Structural health monitoring
Condition monitoring

ABSTRACT

The blades that play a key role to collect wind energy are the most critical components of a wind turbine system. Meanwhile, they are also the parts most susceptible to damage. Structural health monitoring (SHM) system has been proposed to continuously monitor the wind turbine. Nevertheless, no system has yet been developed to a stage compatible with the requirements of commercial wind turbines. Therefore, full-scale structural testing is the main means available so far for validating the comprehensive performance of wind turbine blades. It is now normally used as part of a blade certification process. It also allows an insight into the failure mechanisms of wind turbine blades, which are essential to the success of SHM. Furthermore, it provides a unique opportunity to exercise SHM and non-destructive testing (NDT) techniques. Recognizing these practical significances, this paper therefore aims to carry out an extensive review of full-scale structural testing of wind turbine blades, including static testing and fatigue testing. In particular, the current status in China is presented. One focus of this review is on the failure mechanisms of wind turbine blades, which are vital for optimizing the design of themselves as well as the design of their SHM system. Another focus is on the strengths and weaknesses of various SHM and NDT techniques, which are useful for evaluating their applicability on wind turbine blades. In addition, recent advances in photogrammetry and digital image correlation have allowed new opportunities for blade monitoring. These techniques are currently being explored on a few wind turbine blade applications and can provide a wealth of additional information that was previously unobtainable. These works are also summarized in this paper in order to discover the pros and cons of these techniques.

Contents

1. Introduction

Being a renewable and green source of energy, wind energy has become a pillar of the energy systems in many countries and is recognized as a reliable and affordable source of electricity.

* Corresponding author. Tel.: +86 577 8668 9575; fax: +86 577 8668 9611.
E-mail address: mailtofei@wzu.edu.cn (H.F. Zhou).

http://dx.doi.org/10.1016/j.rser.2014.01.087
1364-0321

It has seen an average growth of 30% in the past decade and the wind capacity doubles every third year. In the year 2012, 100 countries were identified where wind energy was used for electricity generation. In total, the worldwide wind capacity reached 282,275 MW. The contribution of wind energy to the energy supply has reached a substantial share even on the global level: all wind turbines installed around the globe by the end of 2011 contribute potentially 580 Terawatthours to the worldwide electricity supply, more than 3% of the global electricity demand. Furthermore, substantial growth is expected in the future, although the growth in 2012 went down to the lowest rate of 19.1% in the two decades. It is estimated that a global capacity of more than 500,000 MW by the year 2016, and around 1,000,000 MW by the year 2020 are possible [1].

The other side of the coin is that the development of wind energy cannot be smooth sailing all the way. The wind turbines, which convert wind power into mechanical energy and then generate electricity, often operate in harsh environments. Therefore, they may be damaged by many load and environmental factors like fatigue, lightning, fire, strong wind, moisture, and so on. Wind turbine accidents have been reported from time to time. An extensive documentation of wind turbine accidents is provided by Caithness Windfarm Information Forum (http://www.caithnesswindfarms.co.uk) [2]. Fig.1 shows the statistics of wind turbine accidents recorded since 1970s. By September 30 2013, a total of 1446 accidents have been reported worldwide. In trend, more accidents occur as more wind turbines are built. There are an average of 8 accidents per year from 1993 to 1997 inclusive; 33 accidents per year from 1998 to 2002 inclusive; 80 accidents per year from 2003 to 2007 inclusive; and 141 accidents per year from 2008 to 2012 inclusive. The most dangerous failure is a high wind failure, which occurs when the braking system fails, causing the rotor to hit the tower at a high speed. This resulted in considerable damage from parts of the blade to the entire nacelle (rotors attached) flying off the tower structure. Blades and other substantial parts have landed as far away as 500 m in typical cases. For example, the Hedingshan Wind Farm in China's east coastal city of Wenzhou suffered heavy damage after being swept by Typhoon Saomai with wind speeds up to 67 m/s in mid August 2006. Blades suffered the most serious damage. 15 Vestas 600 kW turbines and two Dewind 600 kW units were either fragmented or broken into three parts, while one Vestas 660 kW and two Windey 750 kW machines were toppled. Only eight of the 28 installed wind turbines barely survived.

Although damage can occur to any component or part of the wind turbine, blade failures are a prominent structural failure and are the most common type of damage that occurs in a wind turbine system. According to the accident statistics provided by Caithness Windfarm Information Forum [2], by far the biggest

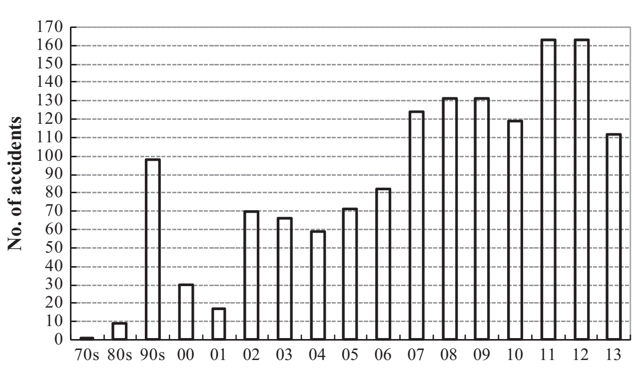

Fig. 1. Statistics of wind turbine accidents recorded since 1970s.

number of incidents found was due to blade failure: a total of 265 separate incidents were found. It has also been shown that the blade damage is the most expensive type of damage to repair and requires considerable repair time. Furthermore, rotating mass unbalance due to minor blade damage can cause serious secondary damage to the whole wind turbine system if prompt repair action is not taken and this can result in the collapse of the whole tower. A failed blade might damage other blades, the tower, the wind turbine itself, and possibly other turbines in the wind farm. Last but not least, the blades are generally regarded as the most critical component of the wind turbine system. The cost of the blades can account for 15–20% of the total wind turbine system [3]. Therefore, utmost care should be given to the wind turbine blades.

To keep wind turbines in continuous operation, structural health monitoring (SHM) of wind turbines is more becoming daily practice. An extensive review of SHM for a wind turbine system has been presented by Ciang et al. [4]. To date, the most successful application of SHM technology has been for condition monitoring (CM) of rotating machinery [5]. Now the CM system has become an integral part of a wind turbine system. The gearbox, bearings, etc. are online controlled with methods derived from CM. Monitoring of these parts is mostly done with accelerometers. Since a lot experience exist in CM, many companies and research institutes worldwide offer their services for monitoring machine parts. The reader is referred to [6,7] for comprehensive reviews of CM of wind turbines. The blade is another most monitored component in a wind turbine system. However, the SHM of wind turbine blades is still in development [8].

So far, full-scale structural testing is the main means available for validating the comprehensive performance of wind turbine blades. It is now normally used as part of a blade certification process. It also allows an insight into the failure mechanisms of wind turbine blades, which are essential to the success of SHM. In addition, it provides a unique opportunity to exercise SHM and non-destructive testing (NDT) techniques in a laboratory environment. The applicability of a big palette of SHM and NDT techniques on wind turbine blades can be tested in the full-scale structural testing. Recognizing these significances, full-scale structural testing of wind turbine blades has been carried out worldwide. A variety of testing procedures, methods, and techniques has been proposed, which usually led to the diversity of testing results. It therefore necessitates a review of these works to help the reader obtain a comprehensive understanding of the full-scale structural testing of wind turbine blades. To the best of the authors' knowledge, reviews in this regard have not been reported yet. This paper therefore aims to carry out an extensive review of full-scale structural testing of wind turbine blades. The review makes a reference database for different testing procedures, methods, techniques, and results, which is beneficial to the reader to enhance their understanding of full-scale structural testing of wind turbine blades. Specifically, a collection of failure mechanisms of wind turbine blades can be used to optimize the design of large-scale wind turbine blades and guide the design of SHM system for them. An assortment of strengths and weaknesses of various SHM and NDT techniques can be employed to evaluate their applicability on wind turbine blades. A collective report of new measurement technologies can help discover their pros and cons as well as indentify promising in-service wind turbine SHM techniques.

The paper is organized as follows. In Section 2, a review of full-scale structural testing of wind turbine blades, including static testing and fatigue testing, is presented. In particular, the current status in China is reported. The failure mechanisms of wind turbine blades are emphasized in this review. Meanwhile, promising SHM and NDT techniques exercised in the full-scale structural

testing are also highlighted. In Section 3, new measurement technologies for wind turbine blade monitoring, including photogrammetry and digital image correlation, are summarized. The key implementation issues as well as the pros and cons of these techniques are discussed. Finally, conclusions and prospects are provided in the final section.

2. Full-scale structural testing

According to IEC 61400-23 [9], the fundamental purpose of a wind turbine blade test is to demonstrate to a reasonable level of certainty that a blade type, when manufactured according to a certain set of specifications, has the prescribed reliability with reference to specific limit states, or more precisely, to verify that the specified limit states are not reached and the blades therefore possess the strength and service life provided for in the design. Furthermore, it must be demonstrated that the blade can withstand both the ultimate loads and the fatigue loads to which the blade is expected to be subjected during its designed service life. In general, blade testing methods fall into two main categories: static testing and fatigue (or dynamic) testing. In static testing, loads are applied statically to the blade and usually in flapwise and lead-lag directions, respectively. In fatigue testing, a loading spectrum containing millions of load cycles are applied. Single-axis tests in flapwise and lead-lag directions are often performed sequentially. Dual-axis testing is another approach, in which both flapwise and lead-lag loads are applied simultaneously. Malhotra et al. presented a good review of the blade testing systems for utility-scale wind turbines [10]. The test load can either be load-based or strength-based. The purpose of load-based test is to show that the blade will sustain the intended loads without failure. This type of test is normally used as part of a blade certification process. Strength-based testing uses as-manufactured blade strength data as its basis, and the blade is tested to failure. This allows a direct verification of the blade strength and failure mechanism, and an assessment of ways in which the design computations, and the resulting design itself, might be improved. This method can be used to find the lowest strength location, relative to expected strength, within a broad region.

2.1. Static testing

Laboratory testing of wind turbine blades was not commonly practiced until 1990s. In 1996, European Commission initiated the European Wind Turbine Testing Procedure Developments (EWTTPD) Project within the Standards, Measurement and Testing Program, to support blade testing laboratories harmonize their testing methods and come closer to a standard set of blade testing procedures [11]. Three European member countries and the United States participated in this project, represented by five laboratories inducing RISØ National Laboratory for Sustainable Energy (RISØ) in Denmark, Center for Renewable Energy Sources (CRES) in Greece, Stevin Laboratory of Delft University of Technology (Delft) in Netherlands, Energy research Centre of the Netherlands (ECN) in Netherlands, and National Renewable Energy Laboratory (NREL) in US. The main objectives were to make a reference database for different test methods, test techniques, and test results of static and fatigue testing of wind turbine blades being used by different laboratories; and to gain a greater collective understanding of the technical challenges of blade testing and to bring the international laboratories closer to a unified approach. Through this project, results from different laboratories may be shared and widely accepted.

The EWTTPD Project laboratories began by selecting a commercial blade model with good design records that could be released to the participating laboratories. The NedWind 25 blade was chosen as the test article, which was a 12 m long blade constructed of glass fiber reinforced polyester. Common static test was prescribed for all the laboratories to determine the blade properties. The mandatory test load was taken to be 75% of the extreme design load. The load application point was at the 7.65 m spanwise location for both flapwise and edgewise loading. In addition, the positions of common strain gauges were also identified, while the laboratories were free to add additional measurement locations at their discretion. The static tests showed reasonable agreement between the different laboratories. Herein, the static tests performed at NREL were cited as an illustration [12]. NREL preformed the static tests at 75% and 110% of the extreme design load for strain verification. A total of 36 strain measurements and 2 bending bridges were used for each blade. Linear behavior was observed in the strain at all loads, indicating no structural failure or buckling stability limits were reached during the static tests.

The fundamental purpose of full-scale static testing is to validate a new blade design. In this regard, a lot of full-scale static testing has been preformed. Nevertheless, only a few tests were available to public due to the proprietary of these works and protection of business secrete. Sandia National Laboratories (SNL) initiated a research program to demonstrate the use of carbon fiber in subscale blades [13]. From this effort, three 9 m designs were created. The first blade set was called CX-100 (Carbon Experimental), and contained a full-length carbon spar cap, a relatively new concept at the time. The second blade design, the TX-100 (Twist-bend Experimental), had the same geometry as the CX-100, but featured a significantly different laminate design. The blade was designed to have passive aerodynamic load reduction by orienting unidirectional carbon 20° off of the pitch axis in the skins from approximately 3.50 m outward. The final blade design named the BSDS (Blade System Design Studies) exhibited a highly efficient structure which included such features as a thin, large-diameter root; flatback airfoils; integrated root studs; and a full-length, constant-thickness, carbon spar cap. One blade from each design underwent static structural testing and was tested to failure. An array of sensors was used in the tests to monitor strain, deflection, load, and acoustic emissions (AE). The AE monitoring system detected not only the locations where damage was occurring, but also incipient global blade failure. The CX-100 blade displayed exceptional stiffness. The blade failed due to panel buckling near max-chord which was likely initiated by a separation between the shear web and low-pressure skin in that region. The TX-100 blade successfully demonstrated twist-bend coupling caused by 20° off-axis carbon in the outboard skins. The TX-100 blade failed at a slightly lower load than the CX-100 blade but in a similar location. The BSDS blade displayed exceptional strength in comparison to the CX-100 and TX-100 designs, surviving to almost three times the target test load. The flat back airfoil feature performed well and did not display non-linear behavior until well after the target test load was reached. A large crack developed between the low pressure skin and the shear web in the bonding joint.

Kong et al. proposed a structural design for developing a medium scale wind turbine blade made of E-glass/epoxy for a 750 kW class horizontal taxis wind turbine system [14]. A prototype blade was manufactured and a full-scale static structural test was then carried out at the simulated aerodynamic loads. The experimental results showed that the designed blade had structural integrity. The predicted mass, spanwise center of gravity, blade tip deflection and first flapwise natural frequency agreed well with the corresponding measured values with 4% error. Furthermore, the measured strain results had good agreement with the analytical results.

Another purpose of full-scale static testing is to gain insight into the failure mechanisms of wind turbine blades. To this end, several full-scale static tests to failure have been reported. Risø carried out a project called "Improved design for large wind turbine blades, based on studies of scale-effects (Phase 1)" from 2001 to 2002 [15–17]. The specific purpose was to study scale effects, in particular to classify the failure modes in wind turbine blades from blades tested to failure, to enhance the understanding of failure in composite structures under compressive loading, and develop approaches for experimental characterization and modeling of adhesive joints under mixed mode (from pure peel to pure shear) loading. The blade used in the test was a 25 m epoxy glass fiber (prepreg) blade. Three different tests to a complete failure of the blade were carried out by using different supports on the blade. During the tests, the structural behavior of the blade was monitored with many sensors. Table 1 summarizes the damage found in the study. They were categorized into seven types. The local deflection was shown to be a good quantity for describing the state of the blade, i.e., how close the blade is to failure (buckling of the flanges and webs). However, the global deflection was not very sensitive to the damages that happen locally. Strain gauge measurements also gave good indication of how close the blade is to a failure by showing non-linear behavior. In addition, the practical benefits of AE monitoring were seen in the three tests, including identification of unwanted damages at load yokes, identification of damages making it possible to stop test and investigate damage and finally identification of how close you are to failure.

In [18], a full-scale 34 m wind turbine blade, made of glass-epoxy pre-greg material, was tested to failure under flap-wise loading. Measurements supported by FE-results showed that debonding of the outer skin was the initial failure mechanism followed by delamination buckling which led to collapse. When the skin debond reached a certain size, the buckling strength of the load carrying laminate became critical and final collapse occurred.

Overgaard et al. [19] carried out a full-scale static flap-wise bending test to collapse on a 25 m wind turbine blade manufactured by layered orthotropic and isotropic materials. The observed progressive first failure event, which led to further progressive damage evolution and finally to the sudden ultimately failure of the blade, was locally originated delamination. This resulted in delaminated laminae with elevated in-plane strain levels due to the diminished local moment of inertia of the compressive flange. Consequently, the first failure event caused an amplified increase of 1.75 in strain level at R0.192 (dimensionless distance from the root end) and a premature failure of the blade. The final failure event eventually occurred when the strain level reached the compressive fiber failure strain at which point the intralaminar stiffness erosion at R0.196 resulted in a complete loss of all structural integrity in the blade.

Last but not least, full-scale static testing was also carried out to examine the applicability of SHM and NDT techniques on wind turbine blades. A big palette of SHM and NDT techniques has been tested on wind turbine blades in a laboratory environment. NREL performed the first SHM testing during the static testing of a 9 m long wind turbine blade [20]. The blade was tested to failure. The final failure occurred at an axial location approximately 37.5% from the root end, which was expected to be the critical regions based on testing of earlier blades. One of the likely precursors to the final failure modes was the local buckling of the shear web. Approximately 30 strain gauges and 20 AE sensors were installed and monitored on the blade. Some nonlinearity in the load strain plot was seen, implying the strain data was an indicator of damage. However, strain was a much localized measurement, a large number of strain gauges would be required to monitor a structure for damage. Stress wave parameters were sensitive to the evolving structural damage occurring in the blade. The amplitude and the waveform of the stress wave signals changed as the load level was increased. Changes in the signal amplitude and relative phase were seen in the received signal, particularly near the final failure of the blade. Nevertheless, measured stress waves were affected by not only the damage in the structure but also the change in curvature of the structure and the strain state in the sensors, actuators, and structure. Three independent methods for damage detection were therefore used to predict if damage would occur to the blade: (i) the resonant comparison method; (ii) the variance method; and (iii) the wavelet pattern recognition method. The results showed that stress wave propagation appears to have a promising potential for the detection of evolving damage in composite structures such as wind turbine blades.

Risø carried out a full-scale static testing on a 19 m long blade to verify the abilities of the different types of sensors and NDT methods [21]. Two types of artificial damages were chosen for the test. The first damage was a notch in the trailing edge to promote laminate failure. The second damage was a failure in the adhesive joint in the trailing edge, i.e., the glue in the joint was removed in a part of the trailing edge. The sensors were strain gauges and AE sensors for the notch in a laminate in the trailing edge and a fiber optic micro-bend displacement transducer for the adhesive failure in the trailing edge. The fiber optic micro-bend displacement transducer was developed utilizing the fact that the propagation of light through an optical fiber may be strongly affected by bending

Table 1
Types of damage observed in [15–17].

Damage type	Damage phenomenon
Type 1	Damage formation and growth in the adhesive layer joining skin and main spar flanges (skin/adhesive debonding and/or main spar/adhesive layer debonding)
Type 2	Damage formation and growth in the adhesive layer joining the up- and downwind skins along leading and/or trailing edges (adhesive joint failure between skins)
Type 3	Damage formation and growth at the interface between face and core in sandwich panels in skins and main spar web (sandwich panel face/core debonding)
Type 4	Internal damage formation and growth in laminates in skin and/or main spar flanges, under a tensile or compression load (delamination driven by a tensional or a buckling load)
Type 5	Splitting and fracture of separate fibers in laminates of the skin and main spar (fiber failure in tension; laminate failure in compression)
Type 6	Buckling of the skin due to damage formation and growth in the bond between skin and main spar under compressive load (skin/adhesive debonding induced by buckling, a specific Type 1 case)
Type 7	Formation and growth of cracks in the gel-coat, debonding of the gel-coat from the skin (gel-coat cracking and gel-coat/skin debonding)

the fiber. Two NDT methods, ultrasonic scanning and X-ray inspection, were also used during the test. The following findings were obtained: (i) by use of strain gauges it was possible to measure changes in strain distribution caused by propagating damages. The necessary number of gauges depends on the size of damage the system was monitoring. (ii) The AE system was very capable of detecting even minor crack propagation. The position and severity of damage source events has been successfully determined using both zonal and linear time-of-flight localization arrays. (iii) The optic fiber micro-bend displacement transducer was capable of determining cracks in adhesive joints (and possible also delaminations). It was at least useable for determining crack sizes corresponding to the distance between each transducer. However, it was very important that the transducer remains attached to the separating surfaces because the crack was detected by the relative displacement. (iv) Both the X-ray and the ultrasonic equipment were capable of locating the damage and determining the size of the damage. The ultrasonic system was well suited for determining the size and location of failure in the adhesive joint and most likely determining the failures. For the laminate damage (the notch in the trailing edge) the resolution of the ultrasonic system was too low to give an accurate position of the crack tip. For this damage type the X-ray technique proved to be very versatile. Used in combination, ultrasonic scanning and X-ray inspection were strong NDT tools for damage detection and localization in wind turbine blades.

In [22], a large number of blade tests were carried out in order to include AE monitoring into standard blade certification tests. A total of ten small blades were tested: six baseline blades and four blades with defects. These 4.5 m long glass/polyester blades were specially designed and produced. The defect types and locations have been selected to represent typical examples of real production defect. The blades were loaded uni-axially in the flapwise direction. On most of the blades, cracks formed in the foam sandwich on the compressive side. AE activity from most of these locations was identified, and the cracks were successfully located. The blades with defect were tested with the aim of following the damage increase. Damage growth and final failure occurred at the defect zones. Damage growth could not be observed visually, but the AE data did indicate that the location of the AE events moved during the test. Furthermore, to automate the evaluation of the massive amount of AE data, a suite of pattern recognition software AEGIS, which used clustering algorithms to separate a collection of AE hits into classes based on their AE features, had been developed. When trained for a specific blade type, the software could be used to grade the structural integrity of various zones on the blade according to user-selectable criteria. The software could act as an early warning system against critical damage developing in specific regions of the blade, enabling more intensive observation of final failure mechanisms. The results from the software evaluation were encouraging.

2.2. Fatigue testing

It is much more difficult to carry out the fatigue testing than the static testing. There are few laboratories throughout the world that have the facility to perform fatigue testing of the wind turbine blades: Risø in Denmark, LM Wind Power in Denmark, CRES in Greece, WMC (Wind Turbine Materials and Constructions Knowledge Center) at Delft University of Technology in Netherlands, NREL in US, LBR&TF (The Texas-NREL Large Blade Research and Test Facility) at The University of Houston in US, WTTC (Wind Technology Testing Center) in US, NaREC (New and the Renewable Energy Center) in UK. Each of these test facilities features independently developed blade testing methods. The reader is referred to [10] for more detailed blade testing systems for utility-scale wind turbines. In addition, a small blade fatigue test system which met the criterion of the IEC 61400-23 has been developed for the small composite wind turbine blades [23]. This fatigue test system was able to test 1–3 m long wind turbine blades with single or multiple samples tested simultaneously. Due to the limited availability of fatigue testing facilities, the number of papers found in the literature that reported the full-scale fatigue testing of wind turbine blades is limited.

Within the EWTTPD Project as mentioned in Section 2.1, each laboratory was also required to perform a fatigue test on the blade [11]. The laboratories independently determined fatigue test loads based on the design data, and then performed the tests using their “business as usual” practices. When possible, the laboratories agreed to follow the principles in IEC 61400-23 to reduce variability in the methods. Again, the fatigue testing performed in NREL was presented here as an illustration. NREL performed single-axis and two-axis fatigue tests [12]. The single-axis test combined equivalent life loading for the flapwise and edgewise spectra into a single resultant load. The two-axis test applied the flapwise and edgewise components independently at a phase angle of 90°. During the single-axis test, two areas of blade damage were observed. The first was a crack that developed at the polyurethane joint interface at the root flange assembly. The crack eventually propagated around the root circular section. This crack did not appear to have immediate structural significance, but it would allow moisture intrusion in the field. The second damaged area was a crack inboard of the maximum chord on the trailing edge. This was in the portion of the span where the blade transitions from an airfoil to a circular root section. After it grew to about 100 mm in length, the crack did not noticeably grow during the remainder of the test. The second crack seemed to develop locally as the curved airfoil section attempted to straighten under load. Similar damage was reported by CRES during their fatigue test. A parallel AE test was conducted during the single-axis fatigue testing [24]. High emissions around the observed root cracking and along the spar between station 2500 and 4200 mm on the compressive surface were detected. The trailing edge crack was not detected because the sensors were not properly positioned to detect this damage. The spar damage was verified during post-mortem sectioning. The same damage was observed in dual-axis test, but the onset of visible damage occurred sooner for the single-axis test.

With the same purpose as the static testing, fatigue testing to failure was also carried out on the 9 m carbon fiber wind turbine research blades as mentioned in Section 2.1 [25]. Throughout the CX-100 blade test, a notable dimple was apparent in the low-pressure skin, at the 1100 mm station toward the trailing edge of the blade. The out-of-plane depth of the dimple progressed during testing. Spanwise surface cracks, formed at the joint of the carbon spar cap and the trailing edge panel, were noted between the 1200 and 1400 mm stations. The test was stopped when these cracks had progressed through the thickness of the skin. The out-of-plane movement of the skin became progressively larger once the crack had fully penetrated the skin. In addition, the stiffness had decreased by approximately 12%, and the lead-lag motion progressively increased. The epicenter of the damage was the interface of the carbon spar cap and the glass/balsa panels. The increased crack length and development of a disbonding between the lower pressure skin and spar cap led to increasing larger out-of-plane panel deformation leading to gross panel buckling. Damage to the TX-100 blade manifested itself as fine gel-coat cracks on the high pressure side, running at an angle of 65° with respect to the spanwise axis. These cracks occurred throughout much of the span of the blade, but were most apparent in the 4000–5600 mm span of the blade. These gel-coat cracks progressed in length and gap width until out-of-plane movement of the skins abutting the crack was apparent. As the length and gap

of the crack increased, the principal axis of the crack front deviated from 65° to 20°, which was the same as the principal direction of the carbon fiber laminate. Once the principal direction of the crack coalesced to the principal direction of the carbon fiber, the crack-length rate and the out-of-plane distortion became progressively larger. The incipient cause of damage to the TX-100 blade was the outboard termination of the spar cap, which ends at the 4500 mm station. The spar cap termination caused a stress riser in the stressed-skin laminate. As it was seen, the fatigue-induced failure mechanism and location was significantly different from those caused by the previous static testing.

During the fatigue testing of the TX-100 blade, several SHM and NDT techniques were exercised [26,27]. The SHM systems were implemented by teams from NASA Kennedy Space Center, Purdue University, and Virginia Polytechnic Institute and State University. In addition, a commercial off-the-shelf AE system was also employed to gather the AE data throughout the test. The diversity of materials in the composite wind turbine blade resulted in challenging acoustic properties for AE system. The acoustic velocities were highly anisotropic, and the acoustic energy attenuation was comparatively high resulting in sensor separation of 0.4 m or less. This resulted in increased uncertainty in locating the AE events. However, the AE system did detect significant AE events early in the test and therefore was a very informative diagnostic tool during the test. NASA Kennedy Space Center implemented a wave propagation based SHM technique by instrumenting the high-pressure side an MFC actuator and three MFC sensors and on the low-pressure side an MFC actuator and two MFC sensors. This SHM system was placed entirely in-board from the maximum chord, where the blade had failed in the previous static testing. Unfortunately, this was not where the blade failed in fatigue. The trains placed on the MFC sensors as the blade was loaded and the blade movement may have blocked the random input signals from the actuators causing erroneous sensor data. All this resulted in noisy data. Purdue University installed an array of high sensitivity triaxial accelerometers, low-frequency capacitive accelerometers, and piezoelectric actuators with force sensors over the surface of the blade to monitor the loading and the blade damage. The in-plane displacement measurements between the damage and root were found to be sensitive to the crack growth and direction. The dynamic features of the blade were sensitive to the variations in ambient temperature. Active diagnostics with the method of virtual forces was sensitive to the damage for in-plane measurements following adjustment for thermal effects. Impact identification was demonstrated with 93% accuracy of the location within 1.3% accuracy of the magnitude. Modal decomposition was an accurate prediction of the excitation mode shapes throughout the test and a practical approach for near real time loading monitoring. Second order harmonics excited by the fatigue system were shown to be on the magnitude of the driving frequency at the tip in the lead-lag and spanwise direction. Virginia Polytechnic Institute and State University developed an impedance-based SHM system consisting of 6-each MFC self-sensing actuators mounted on the blade surface and an impedance analyzer. Baseline readings of the MFC sensors before the fatigue test started showed no peaks and therefore no structural information from 5 to 60 kHz. As expected from the initial baselines, no damage was detected throughout the fatigue test.

Likewise, the detection performance for multiple detectors or test statistics using different active sensing hardware systems in identifying the presence and location of a through-thickness fatigue crack was examined in the fatigue testing of the CX-100 blade [28–30]. In the acquisition hardware domain, the ultrasonic guided wave (UGW) method was compared with the diffuse wave field (DWF) method; in the detector domain, energy methods were compared with correlation methods. The UGW data at a relatively high frequency for fiber glass structures at 200 kHz provided excellent detection performance. At this frequency, the UGW data produced comparable detection performance for both the energy and the correlation methods. Detection performance was best along the spar cap, indicating that for this structure, an extremely low-density array might be sufficient to detect incipient cracks that cross the spar cap. While the 50 kHz UGW data provided good detection performance, the better performing paths lay neither near the crack nor along the spar cap. The DWF data displayed the greatest overall sensitivity using the smaller inner array with the energy-based test statistic, with even heightened sensitivity for sensor paths near the crack. With the DWF data, the inner sensor array experienced a noticeable drop in detection performance for the correlation-based test statistic. Therefore, the energy-based detector outperformed the correlation-based detector, and in some cases, applying the correlation-based detector resulted in serious drops in performance otherwise available with the same data. In addition, the use of auto-associative neural network (AANN) as a novelty detection algorithm was also exercised under the fatigue testing of the CX-100 blade [31]. Frequency response functions extracted by using active sensing measurements were used for the novelty detection methods. The use of AANN as a novelty detection algorithm was shown to be effective in detecting alternate mechanism during the continuous fatigue test. Active sensing measurements combined with novelty detection methods enabled a quantitative and qualitative damage detection even when the system exhibited a range of normal conditions.

In [22], fatigue testing on four of the ten blades as mentioned in Section 2.1 was also performed. The aim of these fatigue tests was to have gradual increasing damage and to be monitored by the AE system in a limited time. The fatigue load was increased in steps to realize failure. The development of a methodology appropriate to fatigue tests was significantly more difficult due to the potentially huge data files and the necessity for limiting the amount of data in some way. As a result, the AE system failed to locate all cracks in the fatigue tests.

2.3. Full-scale testing in China

Rich wind resources and strong support in regulations by the Chinese government have enabled the Chinese wind power industry to grow at a fast speed. China became number one in total installed wind capacity in the year 2010 and maintains the lead ever since. The total installed capacity reached 75,324 MW by the end of 2012, accounting for 26.7% of the global wind capacity [1]. Unsuited to the position of the international wind power industry center, laboratory testing of wind turbine blades is not commonly practiced in China. Perhaps the most significant reason is that the facilities required to test blades does not exist in China. Another main reason may be the considerable high cost of full-scale testing of wind turbine blades. As China has started to export wind turbines to other market, an increase in the number of full-scale testing of wind turbine blades is expected.

Modal testing of wind turbine blades emerged in China at the beginning of 21st century. However, the wind turbine blades tested then were of small scale with lengths of some 1 m usually. Full-scale testing of large-scale wind turbine blades was not seen until recent years. In 2009, a full-scale modal testing of a 38 m long blade for MW wind turbines was performed by Institute of Engineering Thermophysics, Chinese Academy of Sciences [32]. The institute has the largest blade test facility in China, which is capable of testing wind turbine blade with a maximum length of 65 m. The main purpose of this modal testing was to validate the finite element model for the blade and the subsequent numerical

simulation. The numerical simulation was verified by the testing results.

So far, the most comprehensive full-scale testing of wind turbine blades carried out in China was accomplished by Yang et al. [33]. A 40 m long E-glass/epoxy composite wind turbine blade was tested to collapse under flapwise loading in a full-scale static test, in order to gain some understanding and insight to the chain of events leading to the collapse of large-scale composite wind turbine blades. The results showed that the debonding of aerodynamic shells from the adhesive joints was the initial failure mechanism in the facture propagation process. The stress concentration induced by the structure defect caused an initial debonding in the adhesive joints between the aerodynamic shells and the shear webs, and a progressive debonding evolution started with increasing loading. Then, instability phenomena (i.e., local buckling and delamination) and its interaction started and propagated with the progressive debonding evolution. When the combined effect of debonding and local buckling and delamination reached a certain extent, a sudden collapse of the blade occurred.

3. New measurement technologies

Routinely, deformations (strain and displacement) are monitored during the full-scale testing of wind turbine blades. Strain measurement by electrical strain gauges is a common technique. Electrical strain sensing is a well-established mature technology with a range of low cost equipment and sensors available. Electrical strain gauges have become so widely accepted that they dominate the entire strain gauge field. Several types of electrical strain gauge exist including capacitance, inductance, semiconductor and resistance. Among them, the resistance type is the most widely used, while capacitance, inductance and semiconductor types are utilized less frequently. Electrical strain gauges, when correctly installed, have the ability to produce accurate results. However, they suffer from several disadvantages. Electrical strain gauges are prone to non-linearity, hysteresis and zero shift due to cold work of the foil material, poor bond, and viscoelastic effects of the carrier material. They are also susceptible to changes in temperature. Therefore, they are not suited to use over many years.

Monitoring displacement of a wind turbine blade is much more difficult, especially under extreme load and fatigue load conditions. The conventional displacement measurement techniques, such as linear variable differential transducers, micrometer gauge and others, are the so-called contact measurements. The contact measurement is a high-precision measurement for small deformations at discrete points on the object. However, the measurement range is very limited and the measurement system has a complex layout when the number of measured points increases. As a result, it is very difficult to measure the displacement of a large-scale wind turbine blade using the contact measurement in the full-scale range due to the complexity of layout and expensive cost. In addition, more than 10^8 cycles will happen in the expected life cycle of 20 year of a wind turbine blade. The sensor applied in the contact method is prone to failure under the cyclic loading in the full-scale fatigue testing.

Recent advances in photogrammetry and digital image correlation (DIC) have allowed new opportunities for blade monitoring. The primary benefit to using photogrammetry or DIC is that the measurement approach is not limited to identifying the displacement or strain at only a few discrete measurement locations, but instead makes full-field surface measurements possible. These techniques are currently being explored on a few wind turbine blade applications and can provide a wealth of additional information that was previously unobtainable. These works are summarized as follows in order to discover the pros and cons of these techniques.

3.1. Photogrammetry

Photogrammetry is a measurement technique where 3D coordinates or displacements of an object can be obtained by using the 2D images taken from different locations and orientations. The principle of this method is similar to the stereoscopic view of human vision. Two imaging sensors view an object from different positions and perspectives. Using such a stereoscopic camera setup, each point of the object surface is focused onto a specific pixel in the image plane of the respective camera. With the knowledge of the imaging parameters for each camera (intrinsic parameters: focal length, principle point, and distortion parameters) and the relative positions and orientations of the cameras with respect to each other (extrinsic parameters: rotation matrix and translation vector), the 3-D position (coordinate) of each surface point can be calculated. This is done by triangulating the location of each point on the object by calculating the intersection of projected epipolar lines-of-sight defined by each of the images. Although each picture provides 2D information only, very accurate 3D information related to the coordinates or displacements of the object can be obtained by simultaneous processing of these images. The method is sometimes called videogrammetry, which implies that sequences of pictures are used to monitor the dynamic response of an object. The method is also referred to as the stereo-photogrammetry when two or more cameras are used and photogrammetric principles are applied to the synchronized series of images to produce the 3D time series of the targets [34].

The first attempt to apply the photogrammetry technique to a wind turbine was made by Corten and Sabel in 1996 [35]. They performed several vibration measurements on a 2 bladed wind turbine of 10 m diameter while the turbine was in operation. For this purpose, they placed several markers both on the blades and on the tower. Based on the results of the consistency checks, the authors reported that the measurement error was directly related to the size of the observed object or field and in the range of 0.043% (or 1/2500) of the field of view. The authors also reported that photogrammetry would be a very promising method to monitor wind turbine dynamics if the hardware and software technology progressed.

Making use of the state-of-the-art software and hardware, a work similar to Corten and Sabel was carried out by Ozbek et al. recently [36]. They were similar in terms of the reflective round markers and the image post processing method used. The tests were conducted on a pitch controlled, variable speed Nordex N80 wind turbine with a rate power of 2.5 MW. The wind turbine had a rotor diameter and tower height of 80 m. An off-the-shelf system consisting of four Charge-coupled Device (CCD) cameras was used to monitor the dynamic behavior of the wind turbine in operation. The whole wind turbine structure was captured in all the pictures taken which resulted in a very large area (120 m high and 80 m wide) to be viewed by each camera continuously during the entire measurement period. The distance between the camera flash light systems and the wind turbine was 220 m. The markers were made up of retro-reflective materials (1000 times more reflective than the background material) to increase the reflectivity of the target and to provide a better visibility. The first edgewise and first flapwise modes were easily identified from the data obtained from photogrammetry. The random component of the coordinate measurement error was in the range of ± 5 mm or 1/16,000 of field of view. The deformations on the turbine could be measured with an average accuracy of ± 25 mm from a measurement distance of 220 m, which was the overall error including both the systematic and random errors. The maximum

value of the systematic error was found to be in the order of ± 30 mm, being found for the outermost markers (tip markers). Accounting for the random error component in the range of ± 5 mm, the maximum overall error could reach 35 mm for the tip markers.

To overcome the difficulties to paint or place reflective markers on large-scale wind turbine blades, a dot-projected stereo-videogrammetry system was created by Johnson et al. to monitor the surfaces of wind turbine blades during static and fatigue testing [37]. The basic videogrammetry setup consisted of a digital projector and two cameras mounted at different viewing angles, as shown in Fig. 2. The projector generated the markers on the surface of the wind turbine blade, while the cameras captured the images of the blade motion. Microsoft PowerPoint slides with different densities of markers were displayed on the surface of the wind turbine blade through the projector to get the correct grid spacing and size. The videogrammetry system was used on the BSDS blade as mentioned in Section 2 during its static and fatigue testing. The test used 54 coded targets to record the motion of the high pressure surface at maximum chord. Three normalization methods were proposed to construct a non-inertial reference coordinate system to negate the motion of the blade as a whole, so that relative motion of the surface points can be measured. Rotational and translational transformation techniques were devised to convert the spatial data into the common coordinate system attached to the blade. The target data were then used to quantify blade shape changes between each of the epochs. The absolute motion, twist and flap of the blade, as well as the relative motions between the points could be obtained. The system tracked projected targets on the surface of the blade with sub-millimeter accuracy, which allowed small deflections and rotations of the blade to be captured. Using of projected targets also allowed for less preparation time, quick adjustments in the target type and spacing, and it did not interfere with the motion, deformation, or shape of the object.

Recognizing the wind turbine blade experienced simultaneously the small buckling deformation and the large integral deformation, a multi-scale deformation measurement system was developed based on the photogrammetry technique [38–39]. In this system, both the integral deformation of the entire blade and the small-scale deformation of aerodynamic shape were monitored. The system was applied to measure the deformation of the 40 m long E-glass/epoxy composite wind turbine blade during the full-scale static testing as mentioned in Section 2.3.

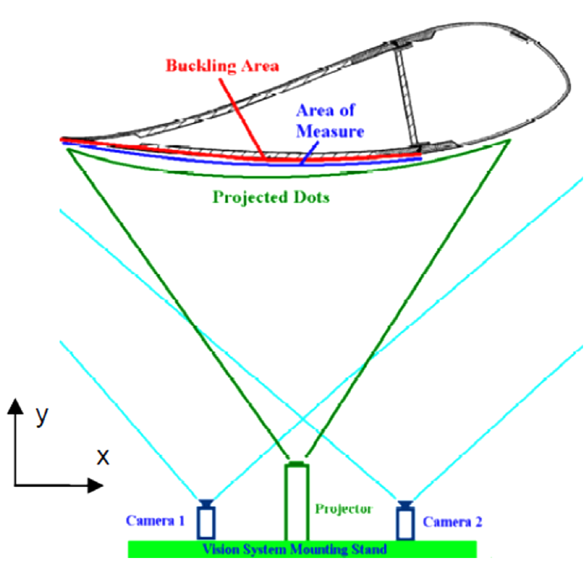

Fig. 2. Dot-projected stereo-videogrammetry system setup [37].

The integral deformation had large amplitude and the measurement required a relatively low precision. In this case, three still cameras were constructed with a large view field and a remote (about 30 m) intersection. Black and white markers were attached to various points for high-precision and sub-pixel location on the image. A parallel network measurement method was proposed for the buckling deformation measurement as relatively high precision was required in this case. The blade was divided into several local sections about 3 m length, and each of interest was measured by a set of stereo cameras. All the sets of stereo cameras were networked in parallel and triggered simultaneously. Grid landmarks were drawn on the blade surface. The results showed that the accuracy of the integral deformation measurement is higher than 0.5 mm per meter. The accuracy of the small-scale deformation measurement is higher than 0.1 mm per meter.

Photogrammetry technique has also been applied to the identification of dynamic characteristics of wind turbine blades. In [40], the stereo-photogrammetry technique was used to identify the mode shapes of a 1.17 m diameter wind turbine blade. The blade containing a handful of optical targets was excited at different frequencies using a shaker as well as a pluck test. The response was recorded using a pair of high speed cameras, and the displacements of the optical targets during the tests were measured using the dynamic point tracking software. The modal frequencies and operating shapes for the first two flapwise bending modes were extracted from the out-of-plane displacements. They were then compared to those extracted from a finite element model and a hammer impact test. Strong correlations among the modes extracted with the three methods were observed, evidencing the capability of stereo-photogrammetry technique in vibration measurements. The stereo-photogrammetry could be used for the measurement of low-frequency vibrations.

Lundstrom et al. improved upon the experimental methods used on the 1.17 m diameter wind turbine blade as mentioned above [41]. These improved methods were applied to a larger 2.56 m diameter turbine/rotor analog, which was composed of three oak planks mounted to a central hub. Operating data on the structure was collected outdoors and shape information was extracted from this operating data. Mode shape extraction proved to be quite difficult because of the low rotation of the structure that resulted in very closely spaced harmonics. The harmonics contribute to the overall response of the structure and obscure the modal parameters and fixed frequency measurements intensive to the system. To remove these harmonics from the structural response, a tachometer signal was developed that output a series of unit pulses synchronized to the x displacement sinusoid and a harmonic filter was computed using the tachometer and applied to the z displacement. The crosspower spectra were computed for the filtered data to extract the mode shapes and frequencies. The operational modes shapes were compared to the mode shapes extracted from the impact measurements using both MAC values and frequencies and these mode shapes were found to compare quite well.

The use of photogrammetry for the measurement of dynamic characteristics of large-scale wind turbine blades has been done by Paulsen et al. [42]. The operating deflection shapes of a 41 m diameter wind turbine were measured during both normal operation, and also an emergency stop. A pair of cameras was placed on tripods approximately 55 m away from each other, and approximately 110 m away from the tower of the wind turbine, resulting in a camera angle of about 30°. The targets had a diameter of 0.3 m in order to meet the 10 pixel diameter requirement for accurate determination of the center-point coordinates. The system provided dynamic deformation data at numerous locations along the length and chord of all blades as well as the tower, such as 3D displacements, operating deflection shapes, blade torsion, tower deformation, etc.

3.2. Digital image correlation

DIC technique relies heavily on the principle of photogrammetry. It uses an arbitrary speckle pattern that is randomly sprayed onto the object surface or that is offered by the texture of the specimen's material. The objective is to obtain an image with a varied and distinctive pattern, in order to enable discrimination between different groups of pixels called subsets. A matching algorithm is employed to recognize and track a specific subset on a series of images. The concept behind the matching algorithm is that the distribution of gray values in a subset of the picture taken at the undeformed state corresponds to the distribution of gray values of the same subset of the picture taken at the deformed specimen. Possible matches at several locations are checked and a similarity score (correlation function) is used to grade them. By tracking the subsets in each successive image and applying photogrammetric principles of triangulation and bundle adjustment, the 3-D position or coordinate of each subset across the surface of the object are obtained and the resulting relative displacements and strains can be calculated. DIC technique was developed in the 1980s independently by Yamaguchi [43] and Peters and Ranson [44]. But the technology has only recently been exploited in industry and research, benefiting from the rapid developments in high resolution digital cameras and computer technology.

The use of DIC technique to measure the full-field stress and strain of wind turbine blades were explored in [45–46]. In preparation for the testing of an actual wind turbine blade, testing and analysis was performed on a 5 ft long aluminum beam. A static test was first performed for the validation of the test setup and methodology for the actual testing. The authors reported that the DIC results and strain gauge data compared very well. All strain measurement between the two techniques had correlation coefficients greater than 0.98, validating the use of DIC for this application. Two different dynamic tests were then performed to study the effectiveness of the DIC technique. The first dynamic test was a pluck test where the tip of the beam was displaced a certain amount, released, and the beam oscillated. In another dynamic test a shaker was located near the base of the beam and oscillated at the first natural frequency of the system. Again, the DIC results and strain gauges data compared very well in both dynamic tests.

In [47], the 3D static responses of two 8 m long wind turbine blades with and without UD layers were measured by an advanced 3D digital optical deformation measuring system. The system recorded the surface of the blade throughout the entire load history using two CCD cameras. In order for the optical system to capture as much of the blade surface as possible, the two cameras were positioned pointing downwards on the blade surface. As an aid, a speckle pattern (black spray paint on a white background) was applied to the surface of the blade. Since the surfaces of the blade section were of a considerable size, a harsher pattern was needed and the best results was obtained by applying dim black spots of a size around $6 \times 6\ \text{mm}^2$ on the surface. Making use of digital image processing, the full-field 3D displacements and surface strains of the object were obtained from the captured digital images.

During the static testing of the CX-100 blade as mentioned in Section 2.1 [13], full-field displacement and strain measurements were extracted using 3D DIC [48]. Measurements were taken at several angles near the blade root, including along the high-pressure surface, low-pressure surface, and along the trailing edge of the blade. The overall results indicated that the DIC approach could clearly identify failure locations and discontinuities in the blade curvature under load. Post-processing of the data using a stitching technique enabled the shape and curvature of the entire blade to be observed for a large-scale wind turbine blade for the first time. The experiment demonstrated the feasibility of the approach and revealed that the technique readily can be scaled up to accommodate utility-scale blades.

The capability of DIC technique for use in a rotating blade has been investigated by Helfrick et al. [49]. A bench test was designed for this purpose. The test object used was a desk fan with 3 blades each measuring 8.9 cm in the radial direction out from the center hub. The test employed a stereo pair of CCD cameras each with a pixel array of 1600×1200 pixels. A stroboscope with a quick flash was employed to illuminate the object as well as prevent motion blur in capturing fast motion. The stroboscope was positioned about 1 m directly in front of the fan facing at a slightly downward angle in order to reduce glare into the cameras. Surface displacements were calculated by subtracting the measured surface shape of the fan in a static condition from the measurements of the fan made while the blades were rotating. The measurements were de-rotated allowing them to be displayed in a rotating coordinate system as a function of fan angle or time. By so doing, a rigid body displacement during operation could be observed.

4. Conclusions and prospects

In this paper, a review of full-scale structural testing of wind turbine blades is presented. The failure mechanisms of wind turbine blades are emphasized in this review. Meanwhile, promising SHM and NDT techniques exercised in full-scale testing are also highlighted. In addition, new measurement technologies for wind turbine blade monitoring, including photogrammetry and DIC, are summarized. The key implementation issues as well as the pros and cons of these techniques are discussed. The following conclusions and prospects are obtained:

(1) Although some efforts have been made in identifying the failure mechanisms of wind turbine blades, well recognized failure mechanisms, which can be used to optimize the design of large-scale wind turbine blade as well as to guide the design of SHM system, has not been achieved. With the advent of new design concepts as well as the increasing size of wind turbine blades, more structural instability phenomena and more complicated failure mechanisms are expected. Therefore, more full-scale structural tests on large-scale wind turbine blades are necessary in order to gain more experiences with practical significance.

(2) Among the various NDT techniques, AE has been most widely exercised in the full-scale testing of wind turbine blades. The method has the potential to be a promising in-service wind turbine SHM technique. It is sensitive to all kinds of damage up to sub-micron size damage and it can locate the damage or impact quite accurately. It has the potential for distinguishing between the damage types as well. To this end, knowledge relating damage types and sensor signals should be established. A next logical step is to use AE as a standard tool in the full-scale testing and approval of new wind turbine blades. The limitation of this method is the number of sensors required and the signal noise during the operation of the wind turbine. It must be investigated whether sensors can operate satisfactory for a long time under real working conditions.

(3) Non-contact measurement technologies will play more and more important roles in the wind turbine monitoring. Photogrammetry and DIC techniques have become competitive alternatives to traditional contact measurement methods. The capability to capture full-field measurements along with its non-contact features has led to their growing use. Photogrammetry has proven to be a very useful tool for the deformation measurement of wind turbine blades. The use for dynamic measurements on both static and rotating wind

turbine blades is also promising. It is well suited for measurement of low-frequency vibrations. Nevertheless, to apply this technique in SHM, its long-term in-field performance is an open question. DIC has been successfully applied to measure the 3D displacements and surface strains of static wind turbine blades. Attempts have also been made to apply this technique to the measurement of 3D displacements and surface strains of rotating wind turbine blades. But more efforts in this regard have to be paid. Having the full-field measurements provides information about structural defects or abnormalities that traditional sensor could only detect if placed at that discrete location. Therefore, the use of DIC in the full-scale testing of wind turbine blades to failure is recommended. Likewise, its application in SHM is much more challenging.

Acknowledgments

The work described in this paper was supported in part by a Grant from the Zhejiang Provincial National Science Foundation of China (Project no. LY12E08009), a Grant from the National Science Foundation of China (Project no. 51208384), and a Grant from the Science Technology Department of Zhejiang Province, China (Project no. 2012R10071).

References

[1] The World Wind Energy Association. World wind energy report. Available from: ⟨www.wwindea.org⟩; 2012.
[2] Caithness Windfarm Information Forum. Summary of wind turbine accident data to 30 June 2013. Available from: ⟨http://www.caithnesswindfarms.co.uk⟩.
[3] Burton T, Sharpe D, Jenkins N, Bossanyi E. Wind energy handbook. New York: John Wiley & Sons; 2001.
[4] Ciang CC, Lee JR, Bang HJ. Structural health monitoring for a wind turbine system: a review of damage detection methods. Meas Sci Technol 2008;19:122001.
[5] Farrar CR, Worden K. An introduction to structural health monitoring. Philos Trans R Soc A – Math Phys Eng Sci 2009;365(1851):303–15.
[6] Hameed Z, Hong YS, Cho YM, Ahn SH, Song CK. Condition monitoring and fault detection of wind turbines and related algorithms: a review. Renew Sustain Energy Rev 2009;13(1):1–39.
[7] Hameed Z, Ahn SH, Cho YM. Practical aspects of a condition monitoring system for a wind turbine with emphasis on its design, system architecture, testing and installation. Renew Energy 2010;35(5):879–94.
[8] Fritzen CP, Kraemer P, Klinkov M. Structural health monitoring of offshore wind energy plants. In: structural health monitoring 2008, Proceedings of the fourth European workshop on structural health monitoring. Lancaster: DEStech Publications; 2002. p. 3–20.
[9] International Electrotechnical Commission. Wind turbine generator systems – part 23: full-scale structural testing of rotor blades. IEC TS 61400-23; 2001.
[10] Malhotra P, Hyers RW, Manwell JF, McGowan JG. A review and design study of blade testing system for utility-scale wind turbines. Renew Sustain Energy Rev 2012;16(1):284–92.
[11] Bulder BH, van Dam J. Blade testing methods. Petten: Energy research Centre of the Netherlands. Report no.: ECN-C-00-055; 2002 April.
[12] Larwood S, Musial W. Comprehensive testing of NedWind 12-meter wind turbine blades at NREL. In: Proceedings of the 19th American society of mechanical engineers (ASME) wind energy symposium. Reno, Nevada, USA; 2000 January 10–13.
[13] Paquette J, van Dam J, Hughes S. Structural testing of 9 m carbon fiber wind turbine research blades. In: Proceedings of 45th AIAA aerospace sciences meeting and exhibit. Reno, Nevada, USA; 2007 January 8–11.
[14] Kong C, Bang J, Sugiyama Y. Structural investigation of composite wind turbine blade considering various load cases and fatigue life. Energy 2005;30(11–12):2101–14.
[15] Sørensen BF, Jørgensen ER, Debel CP, Jensen FM, Jensen HM, Jacobsen TK., et al. Improved design of large wind turbine blade of fiber composites based on studies of scale effects (Phase 1) – summary report. Roskilde: Risø National Laboratory. Report no.: Risø-R-1390 (EN); 2004 September.
[16] Debel CP. Identification of damage types in wind turbine blades tested to failure. Roskilde: Risø National Laboratory. Report no.: Risø-R-1391 (EN); 2004.
[17] Jørgensen ER, Borum KK, McGugan M, Thomsen CL, Jensen FM, Debel CP, et al. Full scale testing of wind turbine blade to failure – flapwise loading. Roskilde: Risø National Laboratory. Report no.: Risø-R-1392 (EN); 2004 June.
[18] Jensen FM, Falzon BG, Ankersen J, Stang H. Structural testing and numerical simulation of a 34 m composite wind turbine blade. Compos Struct 2006;76(1-2):52–61.
[19] Overgaard LCT, Lund E, Thomsen OT. Structural collapse of a wind turbine blade. Part A: static test and equivalent single layered models. Compos A: Appl Sci Manuf 2010;41(2):257–70.
[20] Sundaresan MJ, Schulz MJ, Ghoshal A. Structural health monitoring static test of a wind turbine blade. Golden: National Renewable Energy Laboratory. Report no.: NREL/SR-500-28719; 1999 August.
[21] Sørensen BF, Lading L, Sendrup P, McGugan M, Debel CP, Kristensen OJD, et al. Fundamentals for remote structural health monitoring of wind turbine blades – a preproject. Roskilde: Risø National Laboratory. Report no.: Risø-R-1336 (EN); 2002 May.
[22] Joosse PA, Blanch MJ, Dutton AG, Kouroussis DA, Philippidis TP, Vionis PS. Acoustic emission monitoring of small wind turbine blades. J Sol Energy Eng 2002;124(4):446–54.
[23] Lai FM, Yang SH, Wu JH, Hsueh CT, Yang CC, Wang BH, et al. Development of fatigue test system for small composite wind turbine blades. Proc Eng 2011;14:2003–13.
[24] Beattie AG. Acoustic emission monitoring of a wind turbine blade during a fatigue test. In: Proceedings of 35th AIAA aerospace sciences meeting and exhibit. Reno, Nevada, USA; 1997 January 6–9.
[25] Paquette J, van Dam J, Hughes S, Johnson J. Fatigue testing of 9 m carbon fiber wind turbine research blades. In: Proceedings of 46th AIAA aerospace sciences meeting and exhibit. Reno, Nevada, USA; 2008 January 7–10.
[26] Rumsey MA, Paquette JA. Structural health monitoring of wind turbine blades. In: smart sensor phenomena, technology, networks, and systems 2008, Proceedings of SPIE. Vol. 6933, San Diego, California, USA; 2008 March 10–12.
[27] Rumsey MA, Paquette J, White JR, Werlink RJ, Beattie AG, Pitchford CW, et al. Experimental results of structural health monitoring of wind turbine blades. In: Proceedings of 46th AIAA aerospace sciences meeting and exhibit. Reno, Nevada, USA; 2008 January 7–10.
[28] Park G, Farinholt KM, Taylor SG, Farrar CR. A full-scale fatigue test of 9-m CX-100 wind turbine blades. In: structural health monitoring 2011, Proceedings of the 7th international workshop on structural health monitoring. Stanford, California, USA; 2011 September 13–15.
[29] Taylor SG, Farinholt KM, Jeong H, Jang JK, Park G, Todd MD, et al. Wind turbine blade fatigue tests: lessons learned and application to SHM system development. In: structural health monitoring 2012, Proceedings of 6th European workshop on structural health monitoring. Dresden, Germany; 2012 July 3–6.
[30] Taylor SG, Park G, Farinholt KM, Todd MD. Fatigue crack detection performance comparison in composite wind turbine rotor blade. Struct Health Monit 2013;12(3):253–62.
[31] Dervilis N, Choi M, Antoniadou I, Farinholt KM, Taylor SG, Barthorpe RJ, et al. Novelty detection applied to vibration data from CX-100 wind turbine blade under fatigue loading. In: Journal of Physics: Conference Series 382, modern practice in stress and vibration analysis. Glasgow, UK; 2012 August 29–31.
[32] Mao HJ, Shi KZ, Li HL, Wang JL. Modal testing and numberical simulation of large wind turbine blade. J. Eng. Thermophys. 2009;20(4):601–4 [Chinese].
[33] Yang JS, Peng CY, Xiao JY, Zeng JC, Xing SL, Jin JT, et al. Structural investigation of composite wind turbine blade considering structural collapse in full-scale static tests. Compos Struct 2013;97:15–29.
[34] Mikhail EM, Bethel JS, McGlone JC. Introduction to modern photogrammetry. New York: Wiely; 2001.
[35] Corten GP, Sabel JC. Optical motion analysis of wind turbines. In: Proceedings of European union wind energy conference. Goteborg, Sweden; 1996 May 20–24.
[36] Ozbek, M, Rixen DJ, Erne O, Sanow G. Feasibility of monitoring large wind turbines using photogrammetry. Energy 2010;35(12):4802–11.
[37] Johnson JT, Hughes S, van Dam J. A stereo-videogrammetry system for monitoring wind turbine blade surfaces during structural testing. ASME Early Career Tech J, 8; 2009; 1.1–10.
[38] Sun XY, Yuan Y, Zhu ZK, Zhang XH, Yu QF. Videometric research on deformation measurement of large-scale wind turbine blades. Theor Appl Mech Lett 2011;1(1):011005.
[39] Yang JS, Peng CY, Xiao JY, Zeng JC, Yuan Y. Application of videometric technique to deformation measurement for large-scale composite wind turbine blade. Appl Energy 2012;98:292–300.
[40] Baqersad J, Carr J, Lundstrom T, Niezrecki C, Avitabile P, Slattery M. Dynamic characteristics of a wind turbine blade using 3D digital image correlation. In: health monitoring of structural and biological systems, Proceedings of SPIE, vol. 8348. San Diego, USA; 2012 March 12–15.
[41] Lundstrom T, Baqersad J, Niezrecki C, Avitabile P. Using high-speed stereophotogrammetry techniques to extract shape information from wind turbine/rotor operating data. In: Topics in modal analysis II, vol. 6, Proceedings of the 30th IMAC, a conference on structural dynamics. New York: Springer; 2012. p. 269–275.
[42] Paulsen US, Erne O, Schmidt T., Wind turbine operational and emergency stop measurements using point tracking videogrammetry. In: SEM annual conference and exposition on experimental and applied mechanics. Albuquerque, New Mexico, USA; 2009 June 1–4.
[43] Yamaguchi I. A laser-speckle strain gauge. J Phys E: Sci Instrum 1981;14(11):1270–3.
[44] Peters WH, Ranson WF. Digital image techniques in experimental stress analysis. Opt Eng 1982;21(3):427–31.
[45] Carr J, Baqersad J, Niezrecki C, Avitabile P, Slattery M. Dynamic stress–strain on turbine blade using digital image correlation techniques part 1: Static load

and calibration. In: topics in experimental dynamics substructuring and wind turbine dynamics, vol. 2, Proceedings of the 30th IMAC, a conference on structural dynamics. New York: Springer; 2012. p. 215–220.
[46] Carr J, Baqersad J, Niezrecki C, Avitabile P, Slattery M. Dynamic stress-strain on turbine blade using digital image correlation techniques Part 2: dynamic measurements. In: topics in experimental dynamics substructuring and wind turbine dynamics, vol. 2, proceedings of the 30th IMAC, a conference on structural dynamics. New York: Springer; 2012. p. 221-226.
[47] Berring P, Branner K, Breggreen C, Knudsen HW. Torsional performance of wind turbine blades – part I: experimental investigation. In: sixteenth international conference on composite materials: a giant step towards environmental awareness: from green composites to aerospace. Kyoto, Japan; 2007 July 8–13.
[48] LeBlanc B, Niezrecki C, Avitabile P, Chen J, Sherwood J, Hughes S. Full-field inspection of a wind turbine blade using three-dimensional digital image correlation. In: industrial and commercial applications of smart structures technologies 2011, Proceedings of SPIE, vol. 7979. San Diego, California, USA; 2011 March 6–10.
[49] Helfrick MN, Pingle P, Niezrecki C, Avitabile P. Optical non-contacting vibration measurement of rotating turbine blades. In: Proceedings of the IMAC-XXVII. Orlando, Florida, USA; 2009 February 9–12.